Supporting Information：

Selective hydrogenation of high concentration acetylene over the well-defined crystalline sites of Pd₁Cu₁ and Pd₁Cu₃

Junqi Pei, Yamei Xu, Qiuchen Yang, Ruijun Hou[*]

Beijing Key Laboratory for Chemical Power Source and Green Catalysis, School of Chemistry and Chemical Engineering, Beijing Institute of Technology, Beijing, 100081, People's Republic of China
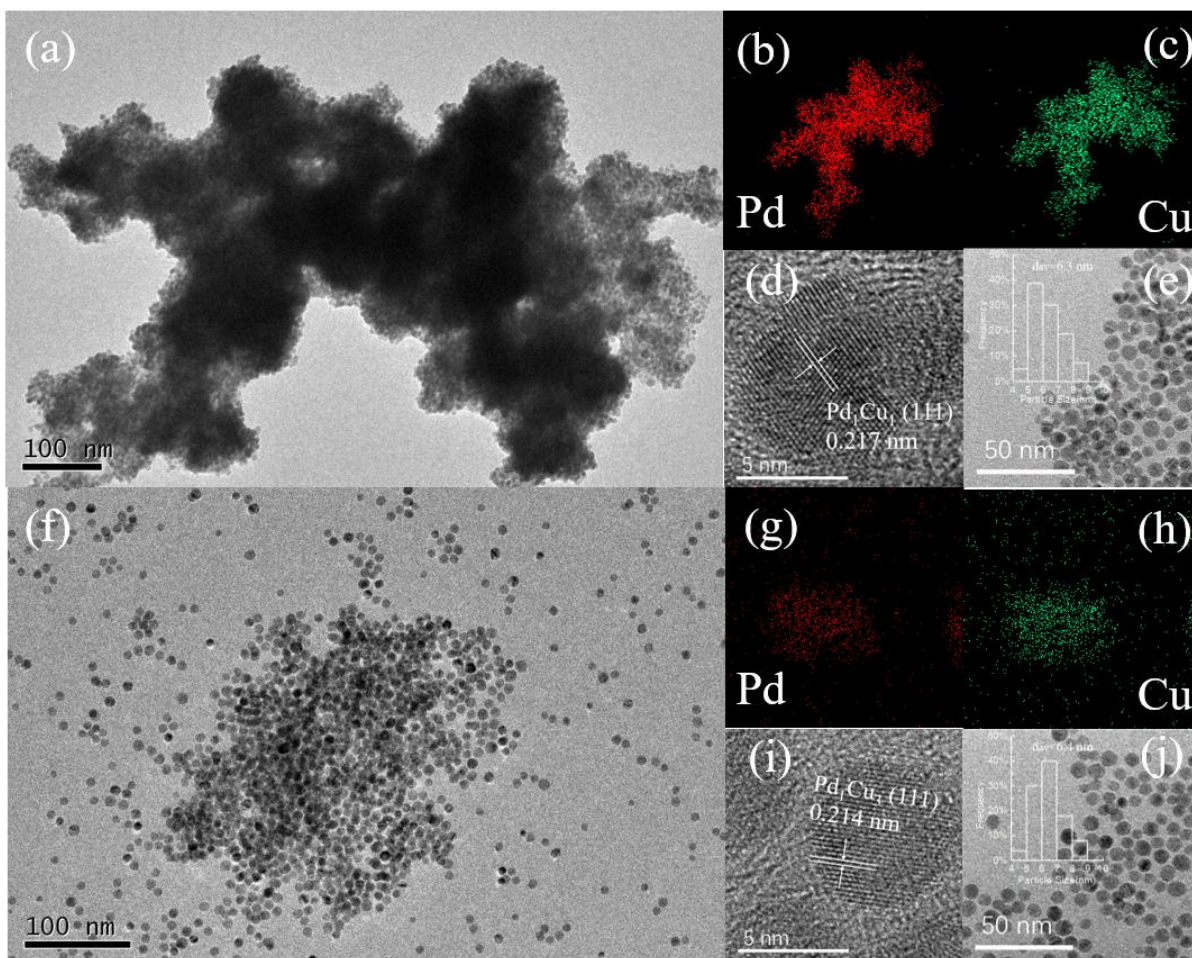
*Corresponding author: hourj@bit.edu.cn

Contents

Figure S1. TEM images and EDS elemental mapping of the unsupported nanoparticles:
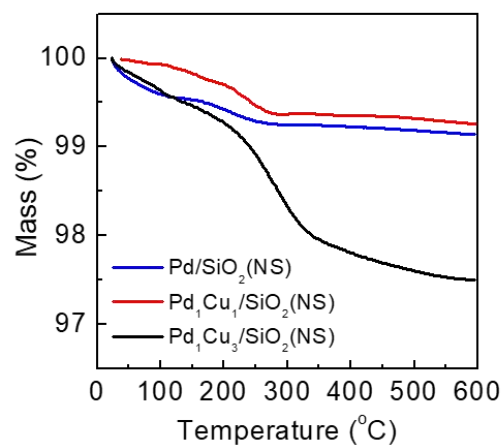(a-e) Pd_1Cu_1(NS) and (f-j) Pd_1Cu_3(NS).

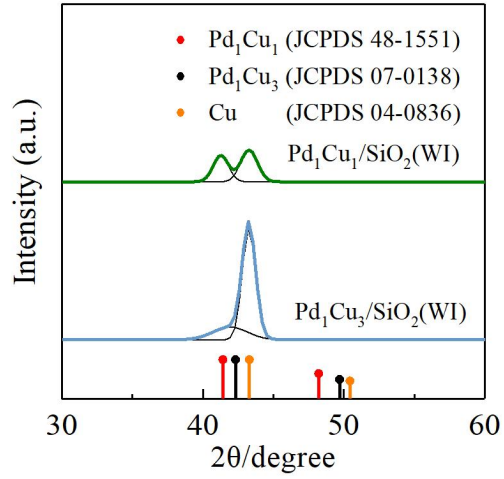Figure S2. TG profiles of the as-synthesized nanoparticles without calcination treatment.

Figure S3. XRD patterns of the PdCu/SiO$_2$(WI) catalysts.

Table S1. XRD peak deconvolution results of the PdCu/SiO$_2$(WI) catalysts.

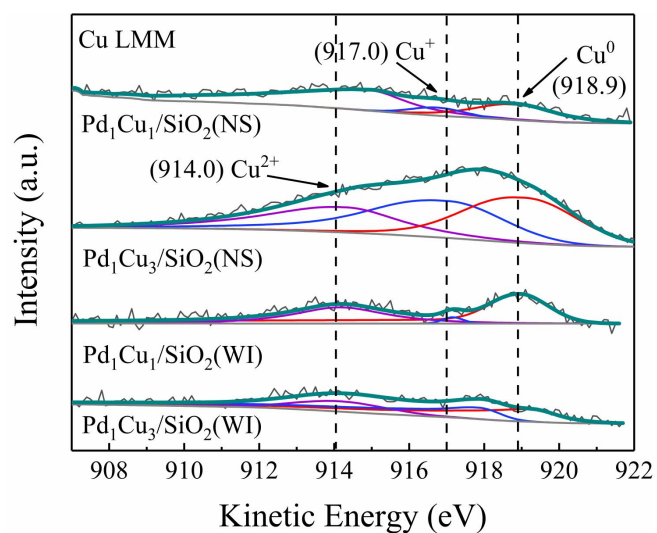|	Alloy phases		Cu	
	Peak position	Area %	Peak position	Area %
Pd$_1$Cu$_1$/SiO$_2$(WI)	41.4 (Pd$_1$Cu$_1$)	43.0	43.3	57.0
Pd$_1$Cu$_3$/SiO$_2$(WI)	42.3 (Pd$_1$Cu$_3$)	23.0	43.3	77.0

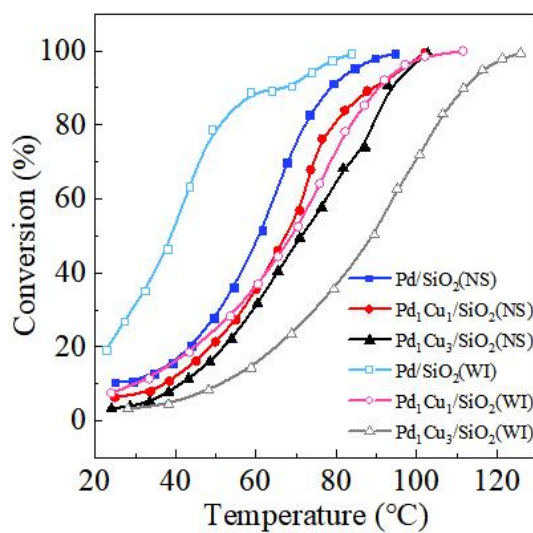Figure S4. CuLMM Auger spectra of the reduced catalysts.

Figure S5. Acetylene conversion as a function of reaction temperature.

Table S2. Ethylene selectivity, TOFs and ln(TOFs) (based on Pd loading and surface site normalization) for different catalysts at low conversions.

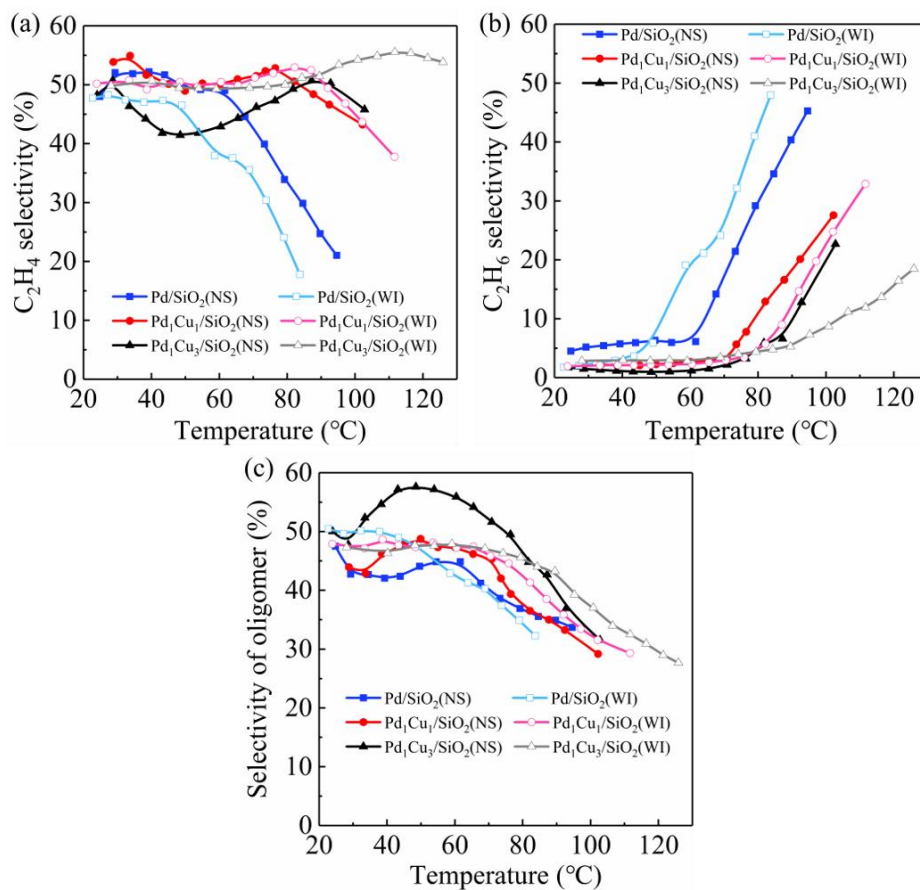| Catalyst	Temperature (°C)	Conversion (%)	C_2H_4 selectivity (%)	TOF/Pd loading (S^{-1})	TOF/ surface site (S^{-1})	ln(TOF)/Pd loading (S^{-1})	ln(TOF)/ surface site (S^{-1})
Pd/SiO$_2$(WI)	22.7	19.2	47.8	0.1	10.5	-1.9	2.3
	26.3	25.0	47.3	0.2	13.7	-1.7	2.6
	31.3	33.2	48.4	0.3	18.2	-1.4	2.9
	32.3	35.2	47.4	0.3	19.2	-1.3	3.0
Pd$_1$Cu$_1$/SiO$_2$(WI)	23.9	7.5	50.2	0.06	2.1	-2.8	0.7
	33.4	11.4	50.8	0.09	3.2	-2.4	1.2
	43.4	18.5	50.3	0.1	5.2	-1.9	1.6
	53.6	28.3	49.7	0.2	7.9	-1.5	2.1
Pd$_1$Cu$_3$/SiO$_2$(WI)	38.2	4.4	50.7	0.03	1.6	-3.4	0.5
	48.2	8.2	49.5	0.06	2.9	-2.8	1.1
	58.8	14.3	50.8	0.1	5.1	-2.2	1.6
	68.9	23.5	49.5	0.2	8.4	-1.7	2.1
Pd/SiO$_2$(NS)	29.3	10.5	51.3	0.2	8.4	-1.6	2.1
	34.4	13.4	50.4	0.3	10.7	-1.4	2.4
	43.9	20.3	51.7	0.4	16.2	-0.9	2.8
	49.1	26.9	50.2	0.5	21.5	-0.7	3.1
Pd$_1$Cu$_1$/SiO$_2$(NS)	28.8	6.1	53.9	0.1	6.2	-2.4	1.8
	38.5	10.7	51.7	0.2	10.8	-1.8	2.4
	45.1	16.2	50.1	0.3	16.3	-1.4	2.8
	55	27.3	50.2	0.4	27.6	-0.9	3.3
Pd$_1$Cu$_3$/SiO$_2$(NS)	28.6	3.9	50.8	0.04	2.0	-3.3	0.7
	38.3	7.8	44.2	0.08	4.0	-2.6	1.4
	48.5	16.0	41.4	0.2	8.1	-1.9	2.1
	53.9	22.1	41.8	0.2	11.2	-1.5	2.4

Figure S6. Selectivity of (a) ethylene, (b) ethane, (c) oligomer at the different temperature in acetylene hydrogenation.
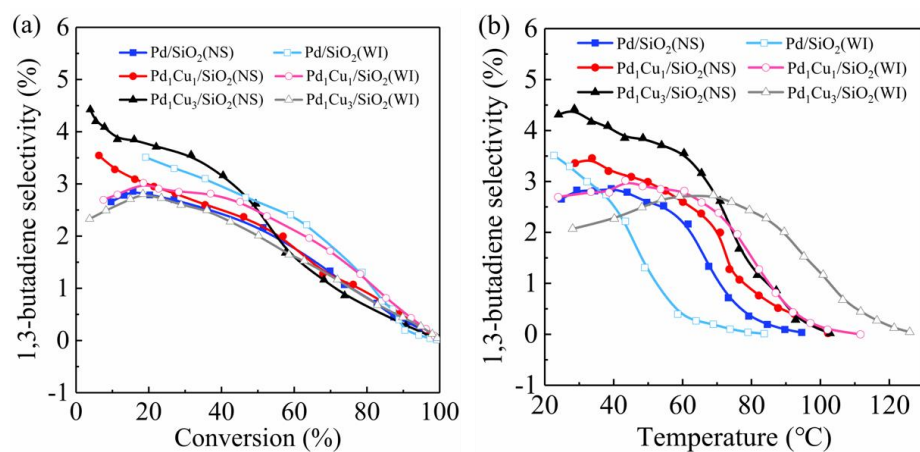

Figure S7. The 1,3-butadiene selectivity over different catalysts with (a) conversion and (b) temperature.
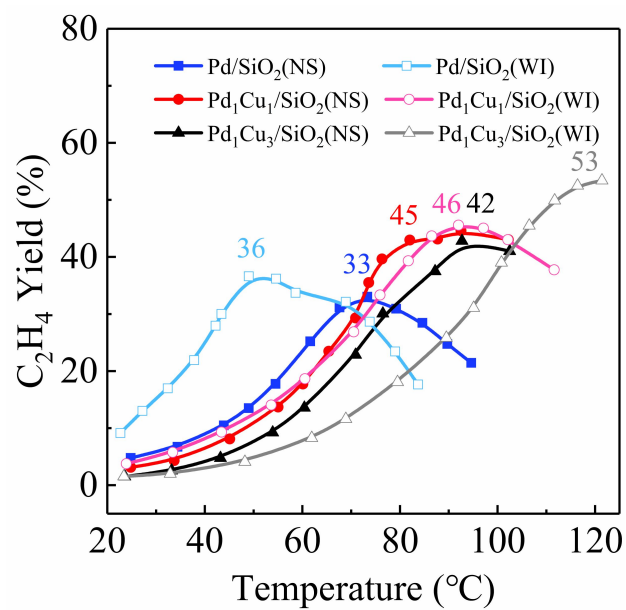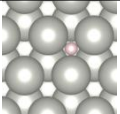
.
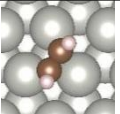
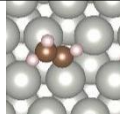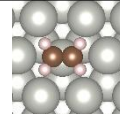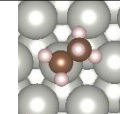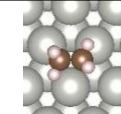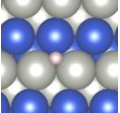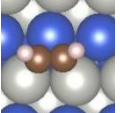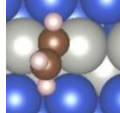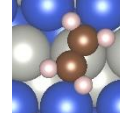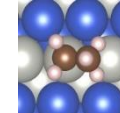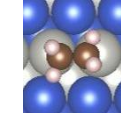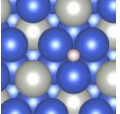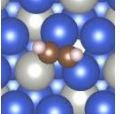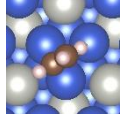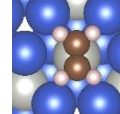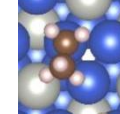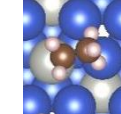Figure S8. Ethylene yield for different catalysts at different reaction temperature.

Table S3. The optimized adsorption patterns of the reaction intermediates on
Pd (111), Pd$_1$Cu$_1$(111), Pd$_1$Cu$_3$ (111) surface.

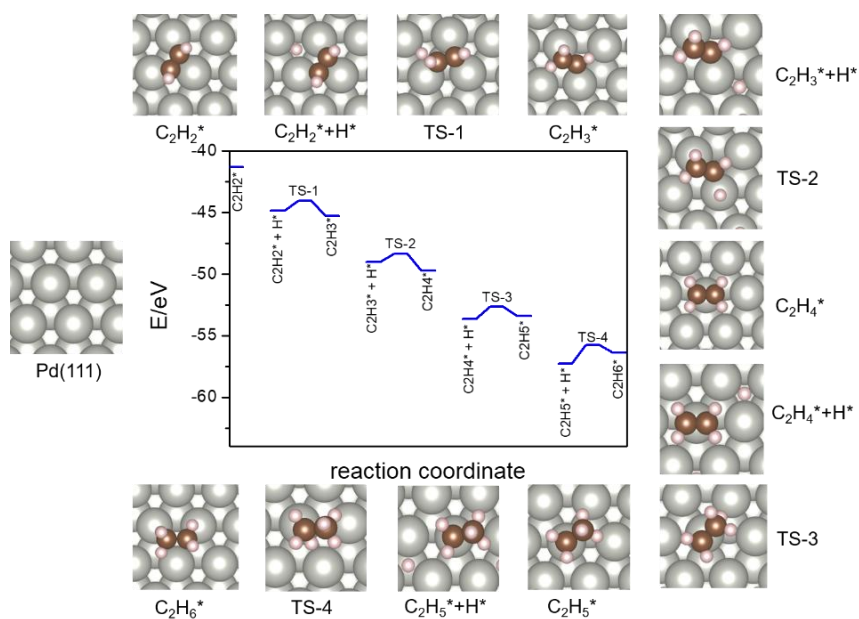|	H*	C$_2$H$_2$*	C$_2$H$_3$*	C$_2$H$_4$*	C$_2$H$_5$*	C$_2$H$_6$*
Pd (111)						
E_{ads} /eV	-2.82	-1.40	-2.37	-0.77	-1.54	1.09
Pd$_1$Cu$_1$ (111)						
E_{ads} /eV	-2.68	-0.78	-2.06	-0.59	-1.56	-0.33
Pd$_1$Cu$_3$ (111)						
E_{ads} /eV	-2.45	-0.50	-1.85	-0.47	-0.98	-0.24

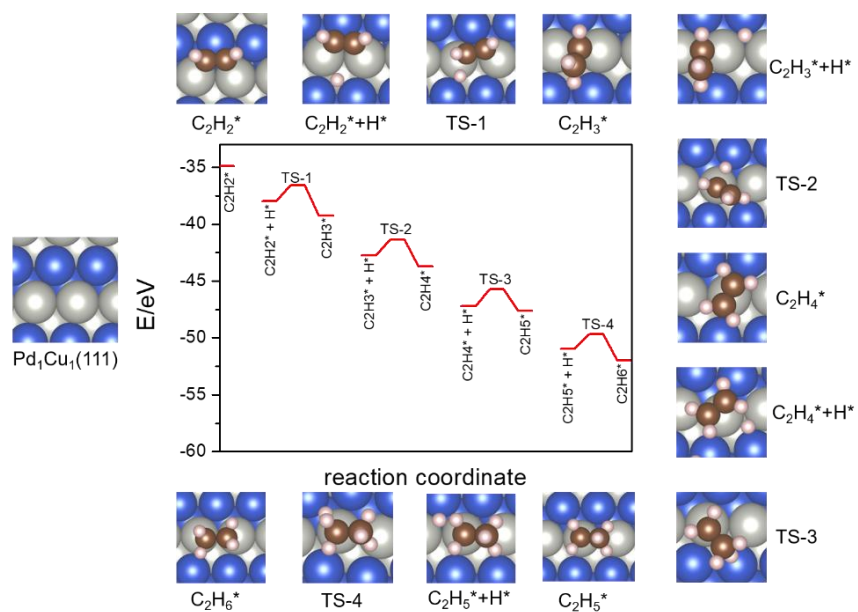Figure S9. The reaction transition states on Pd(111).

Figure S10. The reaction transition states on $Pd_1Cu_1(111)$.

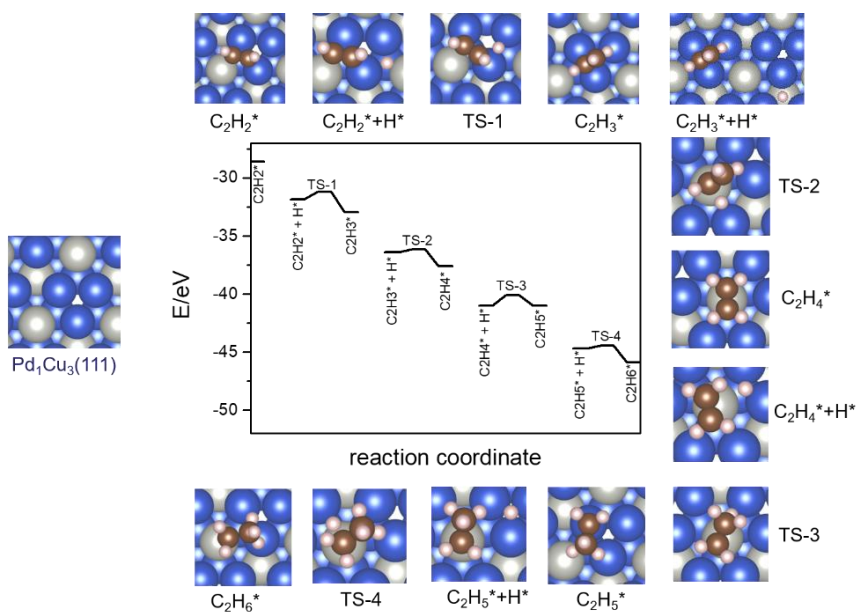Figure S11. The reaction transition states on $Pd_1Cu_3(111)$.